NATIONAL PHYSICAL LABORATORY

AERODYNAMICS DIVISION

AD642149

ON VORTEX STREET WAKES

by

P. W. Bearman

18th April, 1966
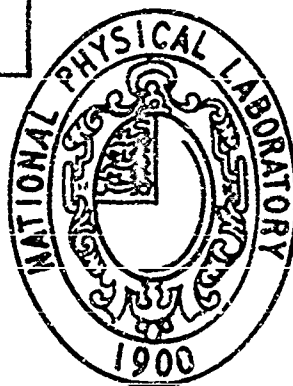
THE RECIPIENT IS WARNED THAT INFORMATION CONTAINED IN THIS DOCUMENT MAY BE SUBJECT TO PRIVATELY-OWNED RIGHTS.

NATIONAL PHYSICAL LABORATORY
1900

DDC

NOV 23 1966

D
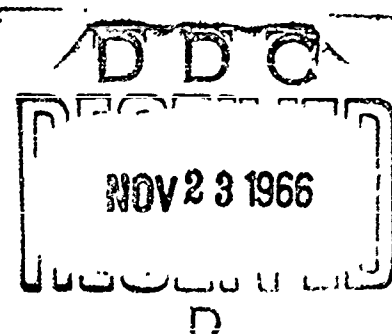
Crown Copyright Reserved

Extracts from this report may be
reproduced provided the source is
acknowledged

A.R.C.28 143

AERONAUTICAL RESEARCH COUNCIL

F.M.3722

FLUID MOTION SUB-COMMITTEE

On Vortex Street Wakes
- By -
P. W. Bearman*

18th April, 1966

A2

*Formerly Cambridge University Engineering Laboratory.

Summary

The flow in the wake of a two-dimensional blunt-trailing-edge model
was investigated in the Reynolds number range 1.3×10^4 to 4.1×10^4. The
effects of splitter plates and base bleed on the vortex street were examined.
Measurements were made of the longitudinal spacing between vortices and
the velocity of the vortices, and compared with values predicted by
von Karman's potential vortex street model. The lateral spacing was
estimated by using both the von Karman and Kronauer stability criteria.
A new universal wake Strouhal number is devised, using the value of lateral
spacing predicted by the Kronauer stability condition as the length dimension.
A correlation of bluff body data was found when pressure drag coefficient
times Strouhal number was plotted against base pressure.

Notation

a	longitudinal vortex spacing
b	lateral vortex spacing
c	velocity of sound
C_{DF}	pressure drag coefficient $\dfrac{D_F}{\frac{1}{2}\rho U_0^2 h}$
C_{DS}	vortex street drag coefficient $\dfrac{D_S}{\frac{1}{2}\rho U_0^2 a}$
C_{DSM}	minimum vortex street drag coefficient
$(C_p)_b$	base pressure coefficient
C_q	bleed coefficient $\dfrac{V_j d}{U_0 h}$
d	bleed slot width
D_F	pressure drag
D_S	vortex street drag
f	vortex shedding frequency
h	base height
h'	distance between shear layers when they become parallel
h"	distance between shear layers at the commencement of vortex formation
K	base pressure parameter, $(C_p)_b = 1-K^2$
ℓ	splitter plate length
N	Shaw acoustic frequency
R_b	Reynolds number based on h, $= \dfrac{hU_0}{\nu}$
S	Strouhal number $= \dfrac{fh}{U_0}$
S_B	new wake Strouhal number $= \dfrac{fb}{U_b}$
S_R	Roshko wake Strouhal number $= \dfrac{fh'}{U_b}$
U_b	velocity at the edge of the boundary layer at separation
U_N	vortex velocity relative to model
U_0	free stream velocity

U_S vortex velocity relative to the free stream

V_j bleed velocity

x distance from base, downstream positive

ρ density

ν kinematic viscosity

suffix k denotes Kronauer stability criterion used

suffix v denotes von Karman stability criterion used

<u>List of Figures</u>

1. Introduction

The aim of this paper is to compare measured vortex street parameters with those predicted by existing theories and to investigate the validity of the vortex street stability criteria of von Karman and Kronauer. It is also intended to investigate how vortex streets are affected by the introduction of either splitter plates or base bleed.

Von Karman (see Milne-Thomson (1938)) represented the vortex street wake, which forms behind a bluff body, by an idealised potential flow model consisting of a double row of staggered point vortices. The associated vortex street drag coefficient C_{DS} can be shown to equal,

$$C_{DS} = \frac{4}{\pi} \left(\frac{U_S}{U_0}\right)^2 \left[\coth^2 \frac{\pi b}{a} + \left(\frac{U_0}{U_S} - 2\right) \frac{\pi b}{a} \coth \frac{\pi b}{a}\right] \quad \ldots (1)$$

where

$$C_{DS} = \frac{D_S}{\frac{1}{2}\rho a U_0^2}$$

D_S is the vortex street drag, U_0 free stream velocity, U_S is the velocity of vortices relative to the free stream, a the longitudinal spacing between vortices and b the lateral spacing between vortices. b/a is often referred to as the spacing ratio.

It has also been shown by von Karman that vortex streets are stable to first order disturbances if $b/a = 0.281$. Substituting this value of the spacing ratio into equation (1) gives

$$C_{DSV} = 1.583 \frac{U_S}{U_0} - 0.63 \left(\frac{U_S}{U_0}\right)^2 . \quad \ldots (2)$$

C_{DSV} can be determined from measurements of the longitudinal vortex spacing and the vortex shedding frequency f. Since $f.a = U_N$, where U_N is the velocity of the vortices relative to the model, and

$$U_0 = U_N + U_S,$$

$$\frac{U_S}{U_0} = 1 - \frac{f.a}{U_0} = 1 - \frac{S.a}{h} \qquad \ldots (3)$$

where $S\left(= \frac{fh}{U_0}\right)$ is the Strouhal number. Conversely, knowing f and vortex street drag, both a and U_N can be predicted.

In his review paper, Wille (1960) pointed out that any array of vortices is unstable to any order of disturbance higher than the first. The arrangement is particularly unstable to any three-dimensional disturbance. It would seem very unlikely, therefore, that vortex streets could possibly exist at high Reynolds numbers where the flow is fully or partly turbulent. The fact that vortex streets do exist casts suspicion on the von Karman stability condition. Various authors, including Timme and Wille (1957) and Berger (1964), have measured values of b/a varying between 0.20 and 0.40 with b/a increasing with distance along the wake.

Kronauer (1964) has shown that spacing ratio is not an important parameter in determining C_{DS}. Figure 1, after Kronauer, shows C_{DS}, obtained from equation (1), against b/a for various values of U_S/U_0. It can be seen that for each value of U_S/U_0, C_{DS} is very insensitive to changes in b/a, the street drag coefficient passing through a broad minimum. Kronauer has proposed a new criterion for stability which states that for a given vortex velocity U_S the vortex street adjusts itself into the configuration giving minimum C_{DS}. The stability criterion can be written as

$$\left(\frac{\partial C_{DS}}{\partial\, b/a}\right)_{\frac{U_S}{U_0} = \text{constant}} = 0 . \qquad \ldots (4)$$

This stability criterion is based on no direct experimental evidence and one of the purposes of this investigation is to determine whether it predicts realistic values of the various vortex street parameters.

In the study of unsteady base flow the most important and least understood parameter is Strouhal number. Many authors have attempted to formulate a universal Strouhal number to compare the wakes of various bluff bodies. The most widely used universal wake Strouhal number is that due to Roshko (1954b). Roshko found, however, that when a splitter plate was introduced into the wake of a circular cylinder the value of his universal Strouhal number depended on splitter plate position. The effect caused by the introduction of wake interference elements on the value of Roshko's wake Strouhal number is investigated further.

2. Measurement of the longitudinal spacing between vortices

2.1 Experimental arrangement

The blunt-trailing-edge models used (fully described in Bearman (1965) and (1966),) had a base height h of 1 in. (2.54 cm) and chord of 6 in. (15.25 cm). The Reynolds number R_b, based on h, was in the range 1.3×10^5 to 4.1×10^5. The nose sections were elliptical and transition wires were attached at 20% chord. One model had provision for fitting splitter plates and the other had a porous base through which air could be bled into the wake. In each case the shear layers leaving the body were parallel and by applying free-streamline theory it can be shown that the pressure drag coefficient, with base height as reference length, is equal to $-(C_p)_b$, the base pressure coefficient.

In Bearman (1965) measurements were presented of S and base pressure coefficient, $(C_p)_b$, against splitter plate length ℓ. Similar quantities were given in Bearman (1966), this time as a function of bleed rate C_q. $C_q = \dfrac{V_j d}{U_0 h}$ where V_j is bleed velocity and d/h is the proportion of the base that was porous. Further experiments are

described here to obtain $^a/h$ as a function of $^\ell/h$ and C_q.

2.2 Experimental procedure and results

The longitudinal spacing 'a' between successive vortices of the same row was measured by using two hot wires. One wire, the reference wire, was fixed at some position in the wake while the second wire, the movable wire, could be traversed along the x axis of the wake. The two resulting signals, after suitable filtering, were displayed on an oscilloscope, one through the X plates and the other through the Y plates, and exhibited the familiar Lissagjou figures. To obtain the steadiest figures it was found that both wires had to be in the same spanwise plane. The upstream wire was positioned a little above the downstream one in order that there should be no interference from its wake.

Typical plots of phase relationships along the wake are shown in figure 2 for the basic model $(^\ell/h = 0$ or $C_q = 0)$, for the model with a splitter plate of length 1.125 h and for the model with a bleed quantity $C_q = 0.0525$. x is the distance of the movable wire from the model trailing edge. The slope of the curve at any position will give the reciprocal of the longitudinal spacing of the vortices at that position. This plot shows that a became constant within 3 or 4 base heights of the model trailing edge. As slope decreases, spacing increases; thus near the model the vortices were much more closely spaced. Very close to the base the signals were so weak that it was impossible to form steady Lissajou figures. As splitter plates were added, or bleed quantity increased, the distance downstream at which steady figures first appeared moved further from the base.

The region in which a was found to be constant will be referred to as the stable region. Figure 3 shows a plot of the stable region vortex

spacing $^a/h$ versus splitter plate length for $R_b = 2.3 \times 10^4$ and
4.1×10^4. From the measurements there appeared to be no consistent
relationship between the two Reynolds number cases but this may have
been due to inaccuracies in measuring $^a/h$. The movable probe could be
positioned to within ± 0.01 h but there was a small range of x over
which the Lissajou figure was observed. This was probably caused by
an unsteadiness in the basic vortex shedding mechanism. The accuracy
in measuring $^a/h$ was limited to about 2 but could have been worse for
the 2.0 h splitter plate where the velocity fluctuations associated with
shedding were comparatively weak.

With knowledge of the shedding frequency and vortex spacing it was
now possible to evaluate U_N, the velocity with which vortices passed
the hot-wire probe.

$$\frac{U_N}{U_o} = \frac{a}{h} \cdot S$$

$\frac{U_N}{U_o}$ evaluated in the stable region is shown plotted in figure 3 against
$^\ell/h$ for the two previous Reynolds number cases. The accuracy is expected
to be no better than 3% since it depends on the accuracy of the measured
values of S and $^a/h$. For the basic model the vortices were travelling
between 88 and 89 of free stream velocity. Since the shedding frequency
was constant down the wake it is evident from figure 2 that in the initial
part of the wake the vortices were accelerating.

Plots of $^a/h$ in the stable region versus bleed rate, for the two
slot widths $(^d/h)$ investigated, are shown in figures 4 and 5. The shape
of these curves is very similar to the shape of the splitter plate curves
in figure 3 with the minimum value of $^a/h$ occurring at the C_q appropriate
to the maximum value of S.

As described in Bearman (1966), over a range of C_q, the hot-wire signals showed very regular fluctuations at frequencies associated with vortex shedding. The resulting Lissajou figures were very steady and the values of a obtained are likely to be more accurate than those found in the splitter plate investigation. In the region of C_q approaching the value where regular shedding ceased the Lissajou figures became very unsteady and hence the accuracy of a deteriorated.

Shown in figures 6 and 7 are plots of U_N/U_o against C_q. It can be seen that there was a general trend towards higher values of U_N/U_o with increasing bleed rate. For the larger slot width values of U_N/U_o greater than unity were recorded at high values of C_q. This would appear to have no meaning and is probably due to the inaccuracy in measuring a, at high values of C_q, mentioned above.

3. Prediction of Vortex Street Parameters

3.1 Vortex velocity and longitudinal spacing

In the introduction the well known potential flow model of the wake was described and the expression (equation (1)) governing the drag associated with such a model was presented. Differentiating this equation and applying the Kronauer stability criterion (equation 4) gives

$$2 \cosh \frac{\pi b}{a} = \left(\frac{U_o}{U_S} - 2 \right) \sinh \frac{\pi b}{a} \left(\cosh \frac{\pi b}{a} - \sinh \frac{\pi b}{a} - \frac{\pi b}{a} \right). \qquad \dots (5)$$

The relationship between b/a and U_S/U_o is shown plotted in figure 8 for values of U_S/U_o up to 0.24. The von Karman stability condition, that $b/a = 0.281$, is also plotted in figure 8 and corresponds to a value of $U_S/U_o = 0.14$, which is a fairly representative value for many bluff body shapes.

As U_S/U_o tends to zero, b/a also tends to zero which suggests a

flow configuration consisting of a line of equal, contra-rotating vortices advancing with zero velocity relative to the free stream. The circulation associated with an individual vortex and the drag of such an array can be shown, from equation (1), to go to zero. The other extreme condition of equation (5) is when $^b/a$ tends to infinity and then $\cosh \pi b/a \approx \sinh \pi b/a$ and $\cosh \pi b/a$. $\sinh \pi b/a$ becomes very much greater than $\pi b/a$. Thus equation (5) becomes

$$\frac{\ddot{U}_2}{U_S} - 2 = \frac{2}{\cosh \frac{\pi b}{a} . \sinh \frac{\pi b}{a}} \rightarrow 0 \qquad \ldots (6)$$

and therefore $U_S = \frac{1}{2}$. This describes the flow in two shear layers where each shear layer is represented by a line of very closely spaced point vortices, such that the distance between the shear layers is very much greater than the longitudinal spacing between successive vortices. Between these two extremes lies the range of values of $^b/a$ for which vortex streets are formed.

For each value of U_S/U_c there is a corresponding value of $^b/a$ which makes C_{DS} a minimum. The minimum vortex street drag coefficient, C_{DS}, is shown plotted in figure 1 against a limited range of values of $^b/a$.

Then equating the vortex street drag to the body drag the problem arises as to whether the vortex street drag should be equated to the body pressure drag or profile drag. With most bluff body shapes skin friction represents a small contribution to total drag. With the basic blunt-trailing-edge section described here skin friction accounted for about 15% of the total drag. This percentage contribution rose to about 30% when a 2h splitter plate was added. The assumption made here is that vortex street drag, derived from the idealised potential flow model of the wake, should be equated to body pressure drag.

In Bearman (1965) and (1966) the effects of wind tunnel blockage on the model drag and base pressure were estimated using the Maskell (1965) correction. This method is only valid, however, up to the position in the wake at which the shear layers become parallel and no detailed information is known about the effects of blockage on the vortex street itself. The drag of the model is to be equated to the drag of the vortex street and thus to be consistent only measured values will be compared.

The body pressure drag coefficient, C_{DF}, can be related to the drag coefficient of the vortex street by

$$h.C_{DF} = a.C_{DS} . \qquad \qquad \ldots (7)$$

Multiplying equation (7) by S gives

$$S . C_{DF} = S . \frac{a}{h} . C_{DS} = \frac{U_N}{U_o} . C_{DS} = F\left(\frac{U_N}{U_o}\right) . \qquad \ldots (8)$$

If either the von Karman or Kronauer stability criterion is used to evaluate C_{DS} the product $S.C_{DF}$ is only a function of the velocity of the vortices. Figure 9 shows a plot of $\frac{U_N}{U_o} . C_{DSM}$ against $\frac{U_N}{U_o}$, where C_{DSM} was obtained using the Kronauer stability criterion. Thus from measured values of S and C_{DF} it is possible to predict $\frac{U_N}{U_o}$. In the following, unless otherwise stated, the Kronauer stability criterion will be used to determine $\frac{U_N}{U_o}$.

It has been shown that, as $\frac{U_N}{U_o}$ tends to 0.5, b/a tends to infinity and therefore all possible values of $\frac{U_N}{U_o}$ must be greater than 0.5. There are two possible solutions of $\frac{U_N}{U_o}$ for values of $\frac{U_N}{U_o}$, C_{DSM} greater than 0.16. It is assumed that the greater of the two solutions always exists, which means that vortex velocities must be greater than about $0.70 \, U_o$. Fage and Johansen (1927) measured $\frac{U_N}{U_o}$ for a large variety of bluff body

shapes and the smallest value recorded was 0.77 U_0. The author knows of no measurements in a fully developed vortex street where $\frac{U_N}{U_c}$ was less than 0.70.

Predicted values of $\frac{U_N}{U_c}$ are shown compared with those measured in the base bleed experiments in figures 6 and 7 for d/h = 0.59 and 0.93 respectively. The theory appears to show the general trend of the results quite well and the agreement is particularly good up to values of C_q of about 0.05. If the theoretical value of $\frac{U_N}{U_0}$ is divided by the experimental value of S, corresponding to that particular C_q, a value for a/h is found. These values are shown in figures 4 and 5 and the agreement between theory and experiment is again close.

The splitter plate results are shown in figure 3 for the two Reynolds number cases. The agreement between the theoretical and experimental values was not so good; the curve of $\frac{U_N}{U_0}$ has an opposite slope to the experimental results for long splitter plates. The reasons for this may lie in the inaccuracy of the experimental results for values of ℓ/h greater than 1.75. The shedding frequency for these long splitter plates was not sharply defined and it may well have been more appropriate to represent S by a band of possible values, corresponding to a band of values for $\frac{U_N}{U_0}$. The values of a/h obtained with the splitter plates are again fairly well predicted by the potential flow model.

The drag of the potential vortex street model, as shown by figure 9, is extremely sensitive to changes in $\frac{U_N}{U_0}$. The drag formula, equation (4), is a function of $\frac{U_S}{U_0}$ and since $\frac{U_N}{U_0}$ is often near unity it is very difficult to measure $\frac{U_S}{U_0}$ very accurately. Taking the basic model as an example; if $\frac{U_N}{U_0}$ changes by 1%, Strouhal number remaining constant, C_{DF} changes by 8%. It is not possible, therefore, within the limits of experimental accuracy, to measure a/h and S and hope to predict

accurate values of C_{DF}. It can be seen that the vortex street parameters need only change very slightly to accommodate large changes in drag. This means that if drag and Strouhal number are known, accurate values of $\frac{U_N}{U_o}$ and $^a/h$ can be predicted.

3.2 Lateral spacing and spacing ratio

As shown by Kronauer (1964) the spacing ratio is not an important parameter in the determination of drag and hence the von Karman drag formula would have predicted the values of $^a/h$ and $\frac{U_N}{U_o}$ equally well. The foregoing work shows, however, that the vortex street model predicts realistic values in vortex streets with wake interference. Use of the Kronauer stability criterion allows predictions to be made of spacing ratio, and also $^b/h$, which may be more representative of the actual flow than the von Karman values.

Figure 10 shows estimations of $^b/h$ and $^b/a$ for the splitter plate results at $R_b = 2.3 \times 10^4$; suffix v denotes the von Karman stability criterion has been used and suffix k the Kronauer criterion. Figure 11 shows the corresponding quantities derived from the base bleed results with $^a/h = 0.93$. It is interesting to note that, for the bleed case, the Kronauer values of $^b/a$ were almost constant up to $C_q = 0.07$. This corresponds to the C_q at which S was a maximum and where there was a kink in the base pressure versus C_q curve described in Bearman (1966). In all cases the von Karman stability criterion predicted higher values of $^b/h$ but the shapes of the curves were very similar.

It is very difficult to measure $^b/h$ experimentally. Berger (1964) states that no characteristic hot-wire signal can be expected from the centres of vortices and criticizes measurements of $^b/h$ that have been obtained by the 'hot-wire technique'. In an attempt to estimate $^b/h$ the flow in the wake of the base bleed model was visualised with smoke.

At high Reynolds numbers it proved very difficult to locate the centres
of vortices and the only conclusion was that $^b/a$ appeared to be less than
0.281 but that it was impossible to assign an accurate value to it. This
in itself, therefore, offers very little proof that $(^b/h)_k$ is more
representative than $(^b/h)_v$. It is proposed, by the introduction of a
new universal Strouhal number, to substantiate that $(^b/h)_k$ is more
representative than $(^b/h)_v$.

3.3 Strouhal number

The only direct attempt to predict Strouhal number has been that by
Shaw (1949), (1951) and (1956) in a series of unpublished papers. Shaw
proposes an acoustic theory which states that the interaction of disturbance
centres, by pulses travelling between them, can exercise a regulating
influence on air flow. He takes as his basic example the flow around a
circular cylinder at subcritical Reynolds numbers. The theory is in good
agreement with experiment but is open to criticism on the grounds that a
suitable mode of vibration has to be chosen. Shaw (1956) extends his
method to various bluff body shapes but is unable to predict a priori
the mode of vibration.

On the basic model described here likely "centres of disturbance" are
the leading edge stagnation point and the two separation points. If it is
assumed that the basic Shaw acoustic frequency N is the one associated
with the passage of a pulse back and forth between the separation points
$N = {}^c/2h$, where c is the velocity of sound. Shaw (1949) shows that

$$S = \tfrac{1}{2}N \frac{U_N}{c} \cdot \frac{h}{U_0}$$

and thus

$$S = 0.25 \frac{U_N}{U_0} .$$

For the basic model $\frac{U_H}{U_c} \approx 0.89$ and the predicted value of S is 0.222 against a measured value of 0.244. Agreement is not as good as Shaw found in the circular cylinder case. The measured value of the longitudinal spacing between vortices was $5.6h$ and by the Shaw analysis a value of $4h$ is predicted.

A pressure transducer was inserted in the centre of the base, flush with the surface, to try and detect any high frequency acoustic waves. Frequency traverses were carried out between 30 c.p.s. and 30 kc.p.s. but the only predominant frequencies were those directly resulting from vortex shedding. Gerrard (1961) was also unable to detect any Shaw frequencies with a pressure transducer flush with the surface of a circular cylinder.

The Shaw analysis assumes that the vortices quickly settle down to a stable configuration. Experimental measurements of U_N/U_J and a/h show this to be true. With the bleed model, if the two rear centres of disturbance are taken as the separation points, the acoustic paths will not change with the addition of bleed and a/h should remain constant. However this is seen not to be the case and a/h decreases by as much as 20% with the addition of bleed. Thus, apart from Shaw's own experiments, there appears to be little evidence to support this theory.

3.4 Wake Strouhal number

It was demonstrated by Roshko (1954b) that, by applying simple physical arguments to the mechanism of vortex shedding, a parameter could be derived to compare the wakes of different bluff bodies. He considered two shear layers a distance h' apart with the velocity outside the layers equal to U_b, the velocity at the edge of the boundary layer at the separation point. The frequency with which vortices were formed was considered proportional to $\frac{U_b}{h'}$ and thus a wake Strouhal

number S_R could be formed where

$$S_R = \frac{fh'}{U_b} .$$

By applying Bernoulli's equation to the flow at the separation point, just outside the boundary layer,

$$U_b = U_0 (1 - (C_p)_b)^{\frac{1}{2}} .$$

It is convenient to replace $(1 - (C_p)_b)^{\frac{1}{2}}$ by K and then

$$S_R = \frac{Sh'}{Kh}$$

h' was obtained by the notched hodograph method (Roshko 1954a) for three simple geometric shapes: circular cylinder, flat plate and 90° wedge. This gave a fairly constant S_R of 0.163 ± 0.01 over most of the Reynolds number range examined.

The notched hodograph method gives the spacing of the shear layers when they become parallel and it is assumed that the vortices begin to form from shear layers with this spacing. With the model shape used to obtain the results described in this paper $h' = h$ and thus $S_R = \frac{S}{K}$. For the basic model this gave a value of $S_R = 0.19$. With the introduction of wake interference it has been shown (see Bearman (1966)) that the vortex formation position is moved further from the body. Thus although h' still equals h, it is no longer representative of the distance between shear layers at the commencement of shedding. For example at $C_q = 0.08$ and $^d/h = 0.93$, $S_R = 0.278$ and thus S_R is not suitable to compare the wakes of bluff bodies with wake interference.

The typical length required will be called h'' and is the distance between shear layers at the commencement of vortex shedding. If the

assumption is now made that the lateral displacement between the vortex rows is equal to h'', a new Strouhal number is obtained. The new Strouhal number S_B becomes

$$S_B = \frac{fb}{U_b} = \frac{Sb}{Kh} .$$

S and K are measured values and b/h can be found by using either the von Karman or Kronauer stability criterion. S_B, found by using the Kronauer stability condition, is plotted against K in figure 12 for the splitter plate and base bleed results, and over the majority of the range a constant values of S_B of about 0.181 was obtained. At low values of K, corresponding to high C_q's and long splitter plates, there was a slight reduction in S_B. This was not surprising because it can be shown that when $K = 1$, S_B will be zero. Taking as an example the basic model shape, it is seen that when $K \rightarrow 1$ (i.e. $(C_p)_b \rightarrow 0$) $C_{DP} \rightarrow 0$. Therefore the vortex street drag will tend to zero and $\frac{U_N}{U_\infty} \rightarrow 1$ which means that the spacing ratio will approach zero. Now since

$$S_B = \frac{fb}{U_b} = \frac{fb}{U_b} \cdot \frac{U_o}{U_o} \cdot \frac{a}{a} = \frac{U_N}{U_o} \cdot \frac{b}{a} \cdot \frac{1}{K}$$

it is clear that S_B will tend towards zero. In the experiments it was found that the wake stabilised and shedding ceased long before $S_B = 0$.

If the von Karman stability criterion had been used to predict b/h a constant value of S_B would not have been obtained. This is demonstrated in figure 12 where $(S_B)_v$ decreases with increasing K. Since S_B involves parameters characteristic of the wake the existence of a constant value of S_B would appear to place some justification on the validity of the Kronauer stability criterion. As a more rigorous test the analysis has been extended to a variety of bluff body shapes.

The information required to compute S_B is the value of C_{DF}, $(C_p)_b$ and S. Circular cylinders have been very well documented by Kronauer (1964) over the Reynolds number range $R_b = 10^2$ to 10^5. Roshko (1961) has carried out experiments at higher Reynolds numbers ($R_b = 2 \times 10^6$ to 10^7) where the boundary layers on the cylinder were turbulent. Flat plate and $90°$ wedge data has been obtained from Roshko (1954b). Further base bleed data was taken from Wood (1964) and Bellhouse and Wood (1965). Fage and Johansen (1927) have published results for an ogival and extended ogival shape and Nash et al. (1963) have presented results for a bluff section fitted with splitter plates. The last two authors only present $(C_p)_b$ and S but in each case the shear layers left the model parallel and free streamline theory has been applied to obtain C_{DF}. The values of S_B for these various bodies are plotted in figure 13 and again show a collapse of the data on to a value of $S_B = 0.181$.

A given value of $C_{DF} \cdot S$, assuming a universal Strouhal number S_B, implies a given value of K. $C_{DF} \cdot S$ is shown plotted against K in figure 14 for all the available data and shows a reasonable collapse of the results. The curve shown in figure 14 was obtained by assuming the Kronauer stability criterion to hold and putting $S_B = 0.181$. The scatter shown in figures 14 would have been greater if profile drag coefficient instead of C_{DF} had been used. By using this correlation of results the vortex shedding frequency of a bluff body can be determined from its pressure distribution.

Although figure 14 shows a general collapse of the data it does not take account of the detailed variations of S, C_{DF} and $(C_p)_b$ at low values of K. As in figure 12 the bleed and splitter plate results show a trend away from the curve $S_B = 0.181$ for values of K less than about 1.16. This value of base pressure corresponds to the value of C_q and ℓ/h

at which S was a maximum. Tood's results also show a trend away from the line $S_B = 0.181$ for values of K less than 1.09. The value of K also corresponds to the C_q at which S was a maximum. Further research is required to determine if there is a change in the vortex formation process at these low values of K.

4. Conclusions

The von Karman idealised potential flow model predicted accurate values of the longitudinal spacing between vortices in the wake behind a two-dimensional blunt-trailing-edge section with and without wake interference. No experimental evidence could be found to support Shaw's acoustic theory of vortex shedding. The value of Roshko's universal wake Strouhal number was affected by the introduction of wake interference elements. Both the von Karman and Kronauer stability criteria were used to estimate the lateral spacing between vortices. Using the Kronauer stability condition to determine b, a new universal wake Strouhal number was formed; $S_B = \frac{fb}{U_b}$. When plotted against the base pressure parameter K, $S_B = 0.181$ over a wide range of K for a variety of bluff body shapes. It is thought that this justifies, in part, the use of the Kronauer stability criterion. From the definition of S_B a universal curve is suggested if $C_{DF} \cdot S$ is plotted against K.

Acknowledgements

References

Bearman, P. W.   1965   Investigation of the flow behind a
                                         two-dimensional model with a blunt
                                         trailing edge and fitted with splitter
                                         plates.
                                         J. Fluid Mech. 21, 241-255.

Bearman, P. W.   1966   Investigation into the effect of base bleed
                                         on the flow behind a two-dimensional model
                                         with a blunt trailing edge.
                                         Paper to be presented at the AGARD
                                         Specialists' meeting on "Separated Flows',
                                         von Karman Institute for Fluid Dynamics,
                                         Rhone-Saint-Genese, Belgium, 10-13th May, 1966.

Bellhouse, B. J. and   1965   The upstream influence of base bleed on
Wood, C. J.   surface pressures and skin friction.
                                         J. R. Aero. Soc. 69, 789-791.

Berger, E.   1964   Die Bestimmung der hydrodynamicschen
                                         Größen einer Karmanschen Wirbelstraße aus
                                         Hitzdrahtmessungen bei kleinen Reynoldsschen
                                         Zahlen.
                                         Z. Flugwiss. 12, 41-59.

Fage, A. and   1927   The structure of vortex sheets.
Johansen, F. C.   Aero. Res. Cou. Lond; R. & M., No. 1143.

Gerrard, J. H.   1961   An experimental investigation of the
                                         oscillating lift and drag of a circular
                                         cylinder shedding turbulent vortices.
                                         J. Fluid Mech. 11, 244-256.

Kronauer, R. E.   1964   Predicting eddy frequency in separated wakes.
                                         Paper presented at the I.U.T.A.M. symposium
                                         on concentrated vortex motions in fluids,
                                         University of Michigan, Ann Arbor, Michigan,
                                         6-11th July, 1964.

Maskell, E. C.   1965   A theory of the blockage effects on bluff
                                         bodies and stalled wings in a closed wind
                                         tunnel.
                                         Aero. Res. Coun. Lond., R. & M., No. 3400.

Milne-Thomson, L. M.   1938   Theoretical Hydrodynamics,
                                         Macmillan and Co. Ltd.

Nash, J. F., Quincey, V. G.   1963   Experiments on two-dimensional base flow at
and Callinan, J.   subsonic and transonic speeds.
                                         Aero. Res. Coun., Lond., Rep. No. 25,070.

Roshko, A.   1954a A new hodograph for free-streamline theory.
                                         Nat. Adv. Comm. Aero., Wash., Tech Note,
   No. 3168.

Roshko, A.	1954b	On the drag and shedding frequency of two-dimensional bluff bodies. Nat. Adv. Comm. Aero., Wash., Tech. Note, No. 3169.
Roshko, A.	'361	Experiments on the flow past a circular cylinder at very high Reynolds number. J. Fluid Mech. 10, 345-356.
Shaw, R. A.	1949	The solution of the problem of a cylinder shedding a periodic wake. Aero. Res. Coun., Lond., Rep. No. 12,696.
Shaw, R. A.	1951	A preliminary investigation of the acoustic theory of air-flow. Low speed wind tunnel tests on an aerofoil and a cylinder. Aero. Res. Coun., Lond., Rep. No. 13,795.
Shaw, R. A.	1956	An explanation of vortex shedding on the basis of pulses travelling at the speed of sound. Aero. Res. Coun., Lond., Rep. No. 18,455.
Timme, A. and Wille, R.	1957	Über das Verhalten der Virbelstraßen. Jb. schiffbautech. Ges. 51, 215-221.
Wille, R.	1960	Karman Vortex Streets. Advanc. appl. Mech. VI, 273-287.
Wood, C. J.	1964	The effect of base bleed on a periodic wake. J. R. Aero. Soc. 68, 477-482.

FIG. I
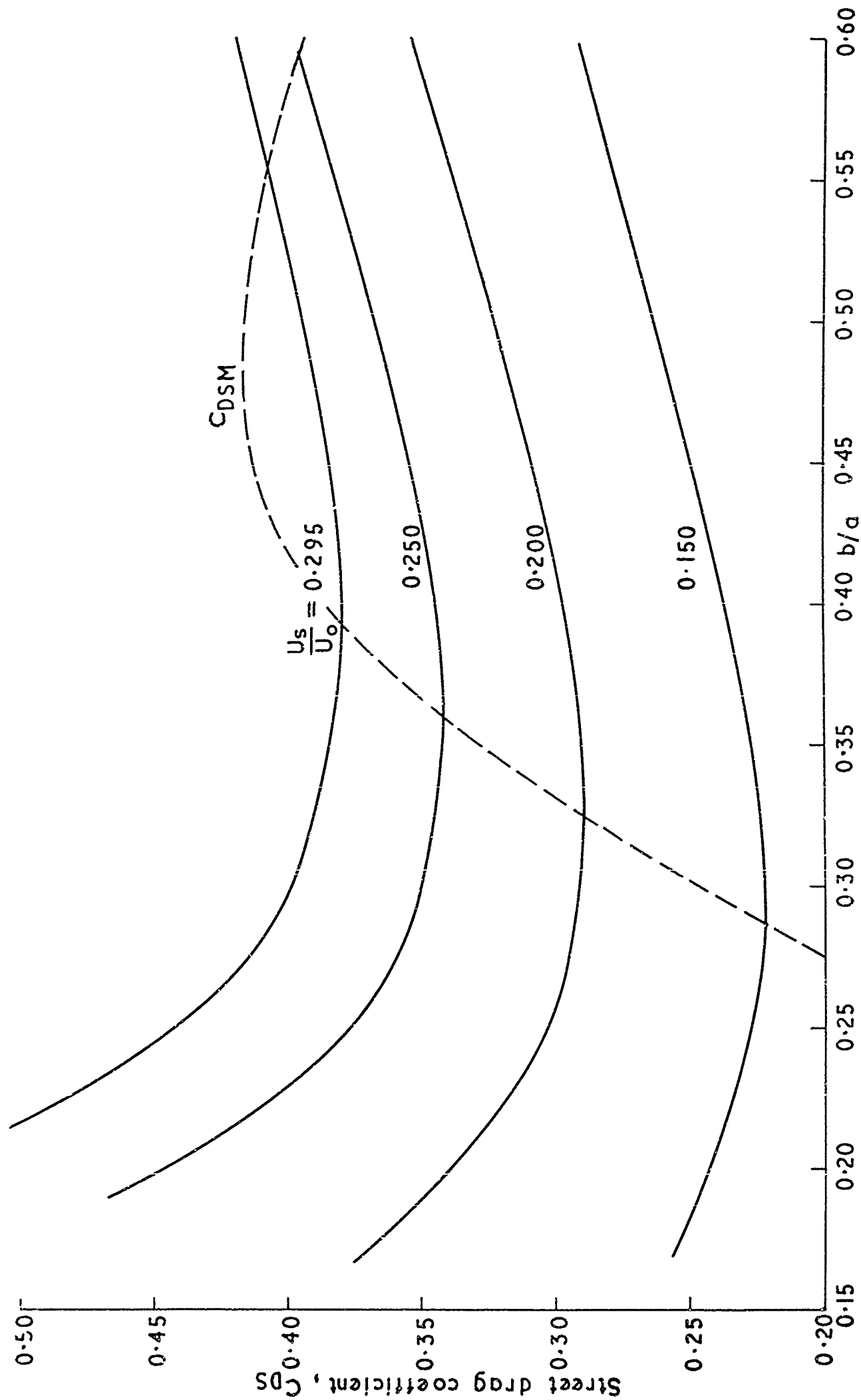
C_{DS} versus b/a for various values of U_s/U_o (after Kronauer (1964))

FIG. 2
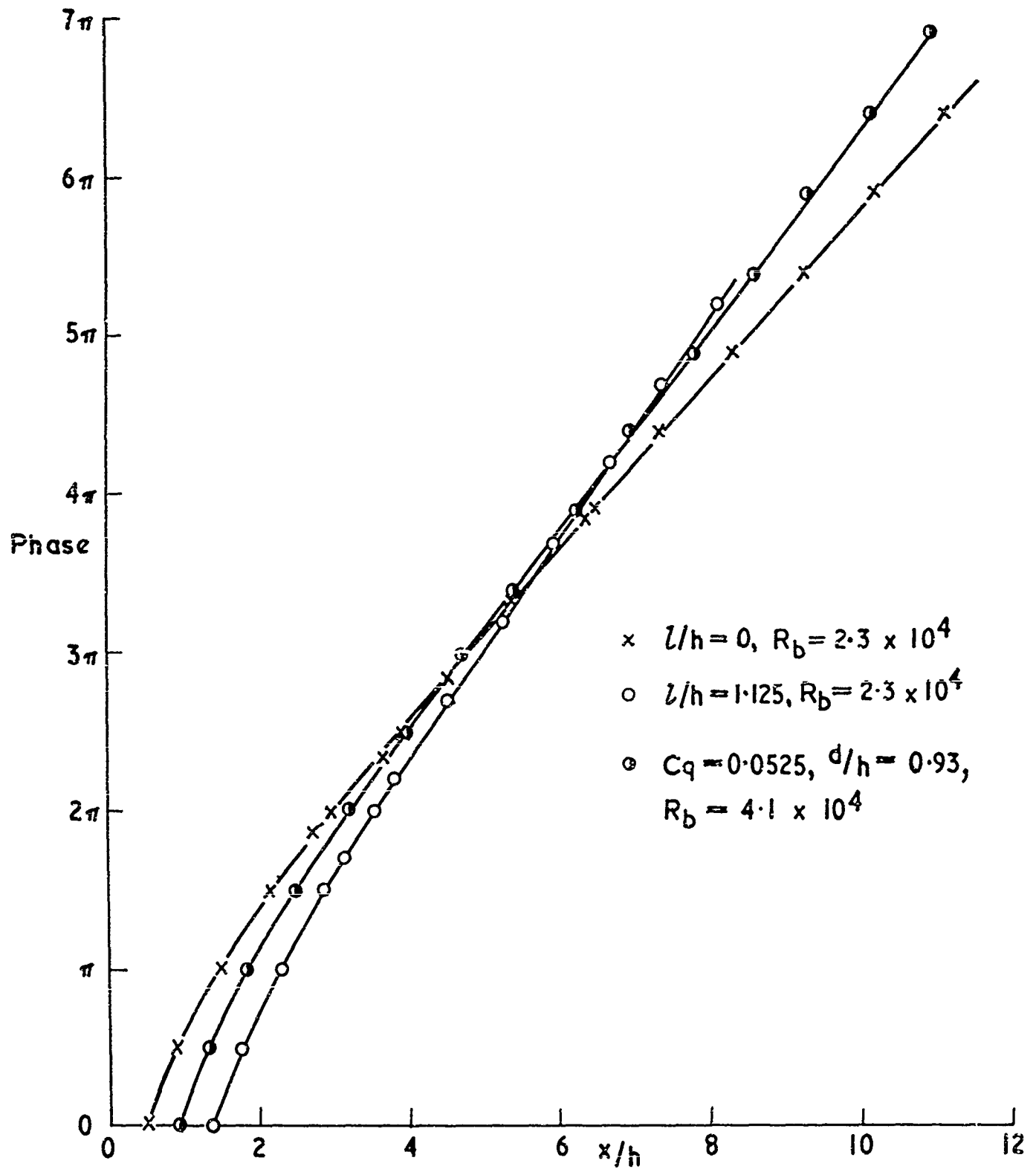
Phase relations along the wake
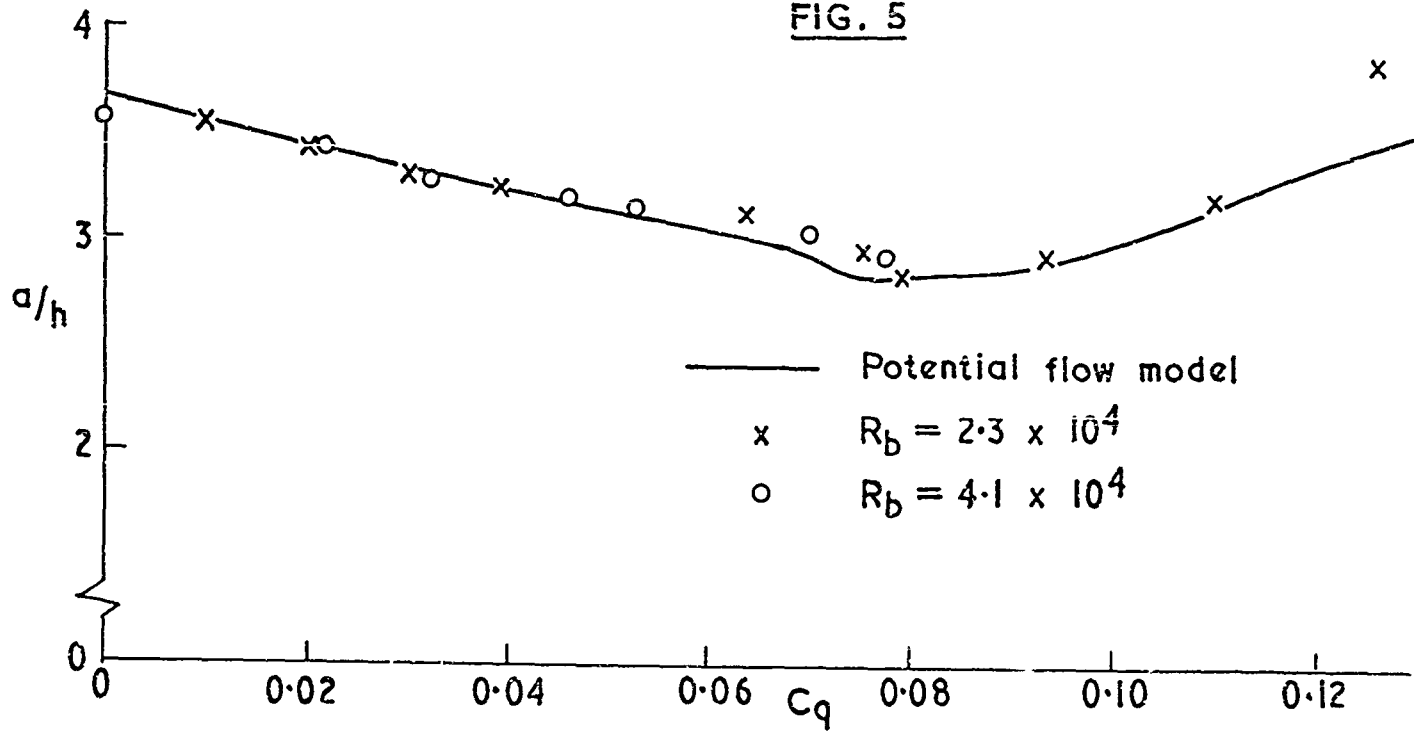
FIG . 3
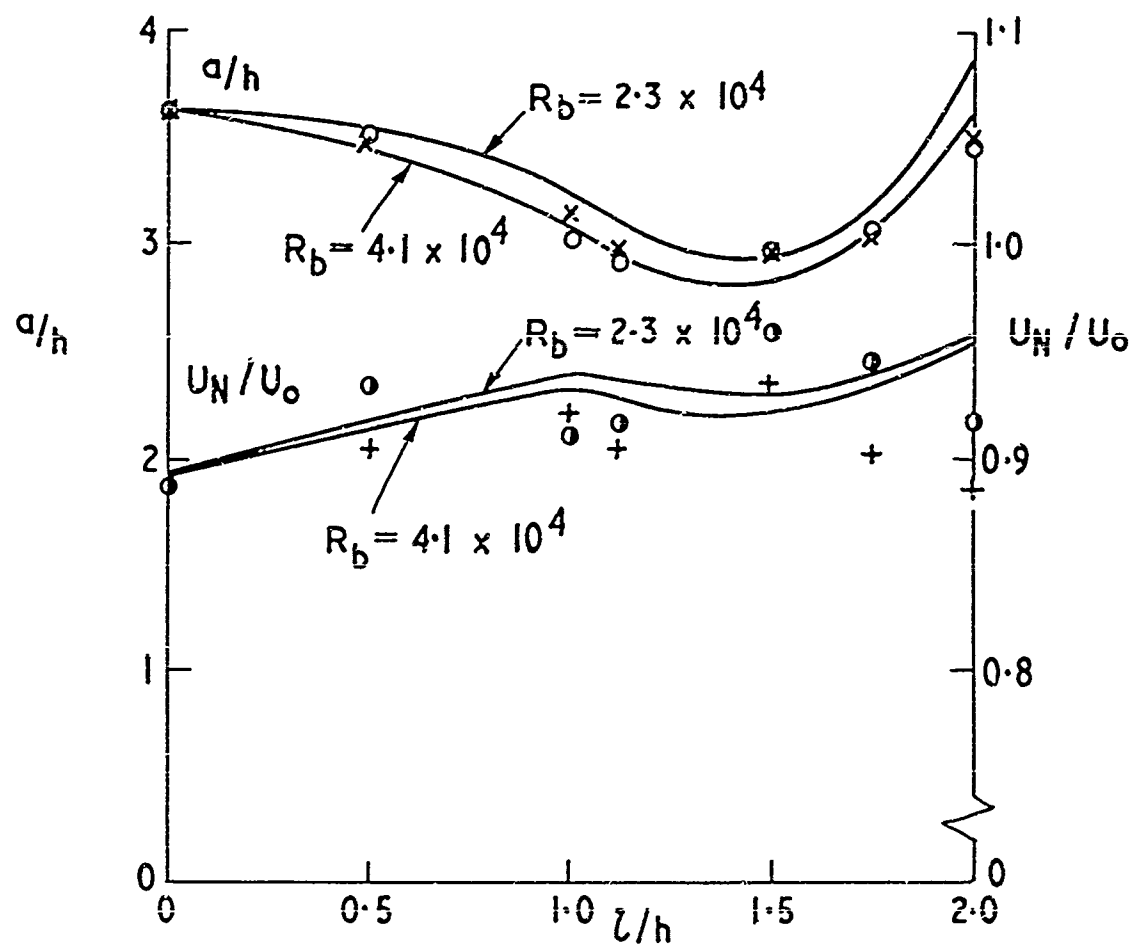
a/h and U_N/U_o versus splitter plate length

FIG. 4
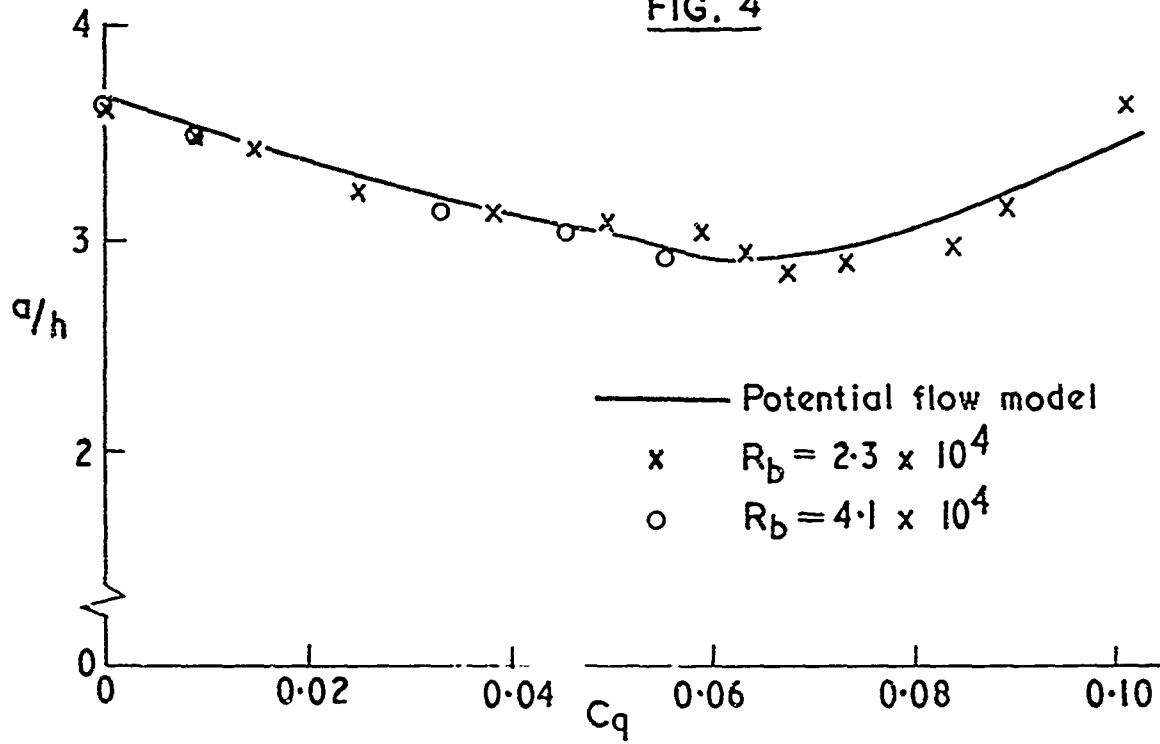
$^a/h$ versus bleed rate, $^d/h = 0.59$
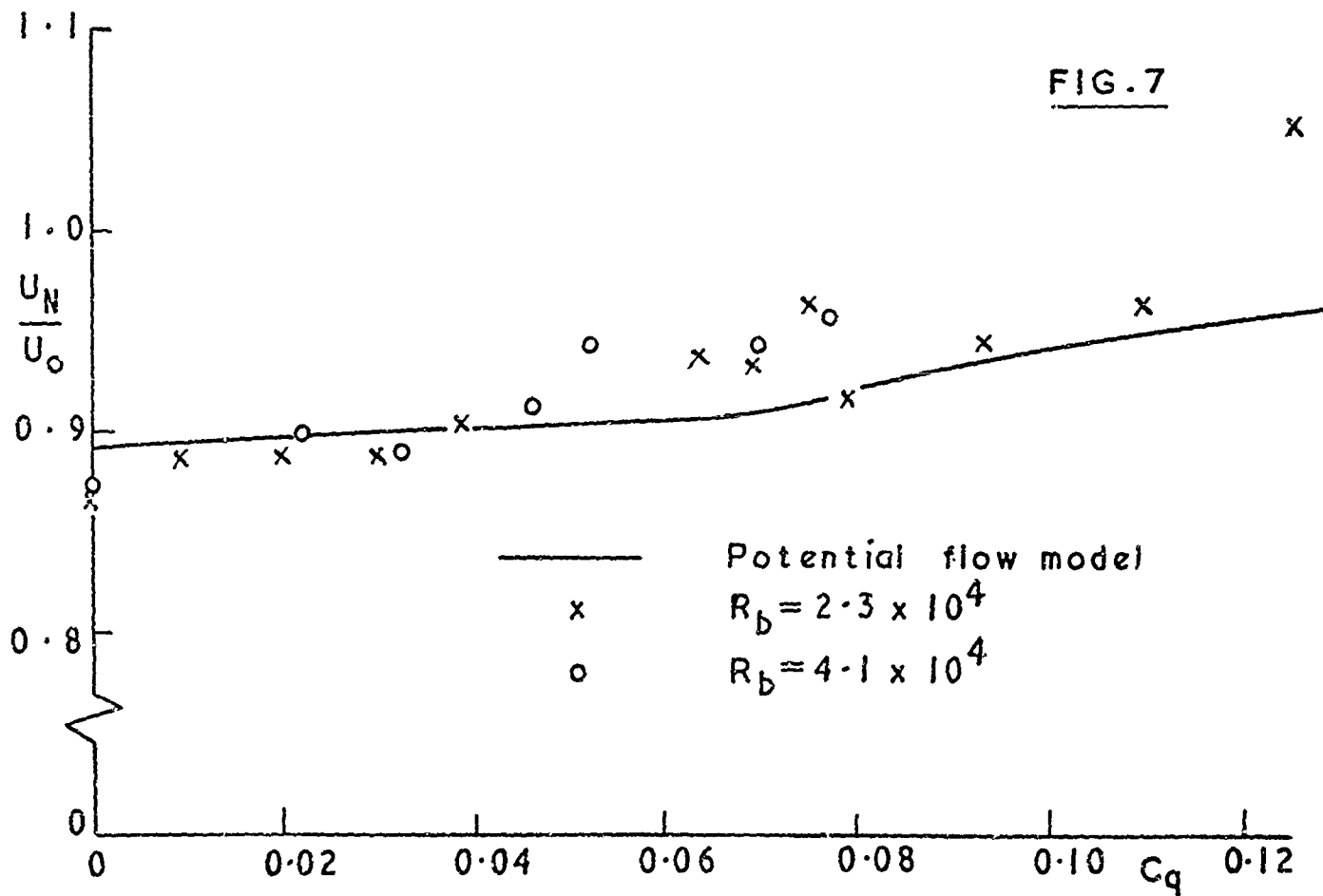
FIG. 5

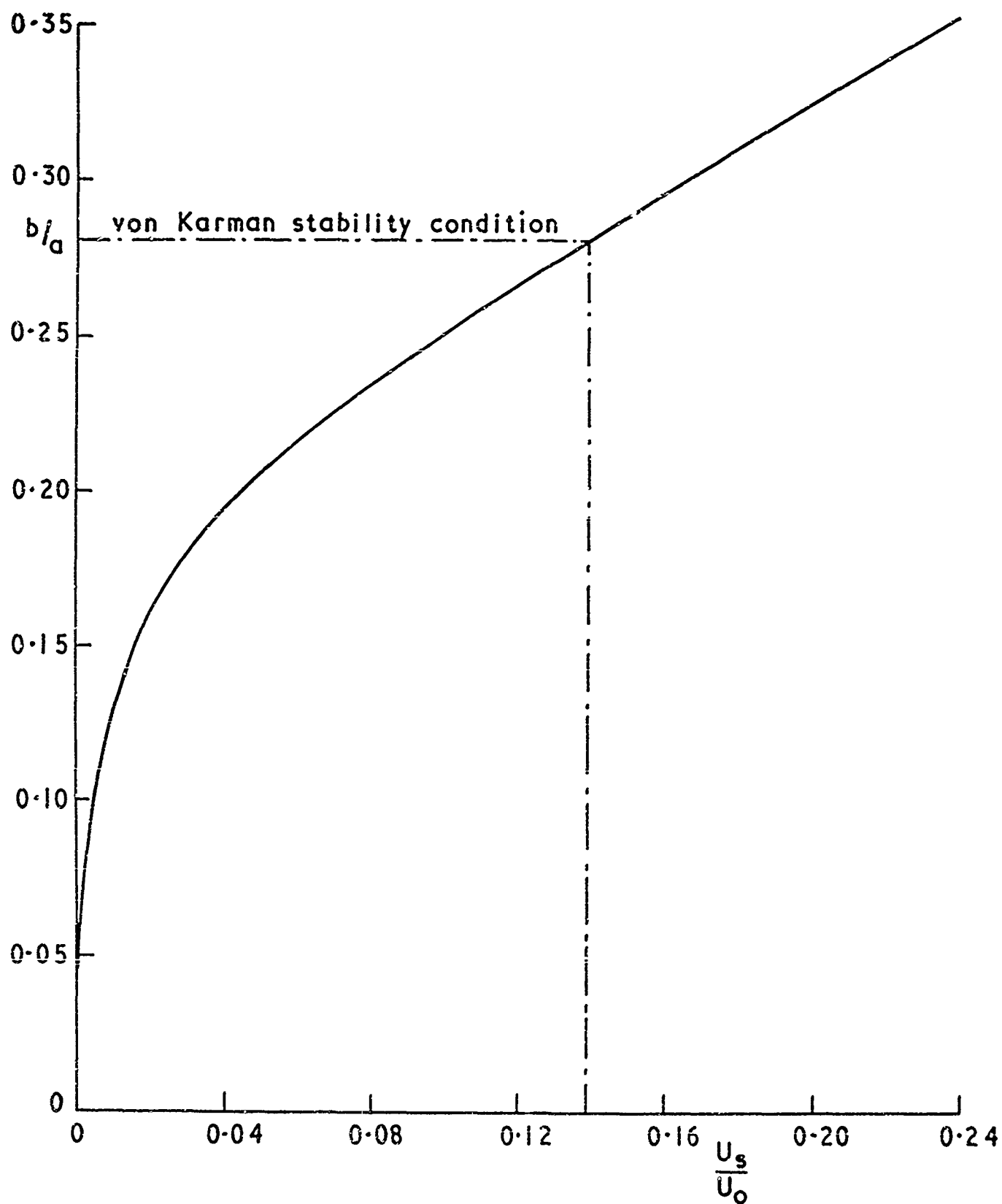$^a/h$ versus bleed rate, $^d/h = 0.93$

FIG.6

$\dfrac{U_N}{U_o}$

1·0

0·9

0·8

0

0   0·02   0·04   0·06   0·08 C_q 0·10

—— Potential flow model

x $R_b = 2\cdot3 \times 10^4$

o $R_b = 4\cdot1 \times 10^4$

U_N / U_o versus bleed rate, $d/h = 0\cdot59$

FIG.7

$\dfrac{U_N}{U_o}$

1·1

1·0

0·9

0·8

0

0   0·02   0·04   0·06   0·08   0·10 C_q 0·12

—— Potential flow model

x $R_b = 2\cdot3 \times 10^4$

o $R_b = 4\cdot1 \times 10^4$
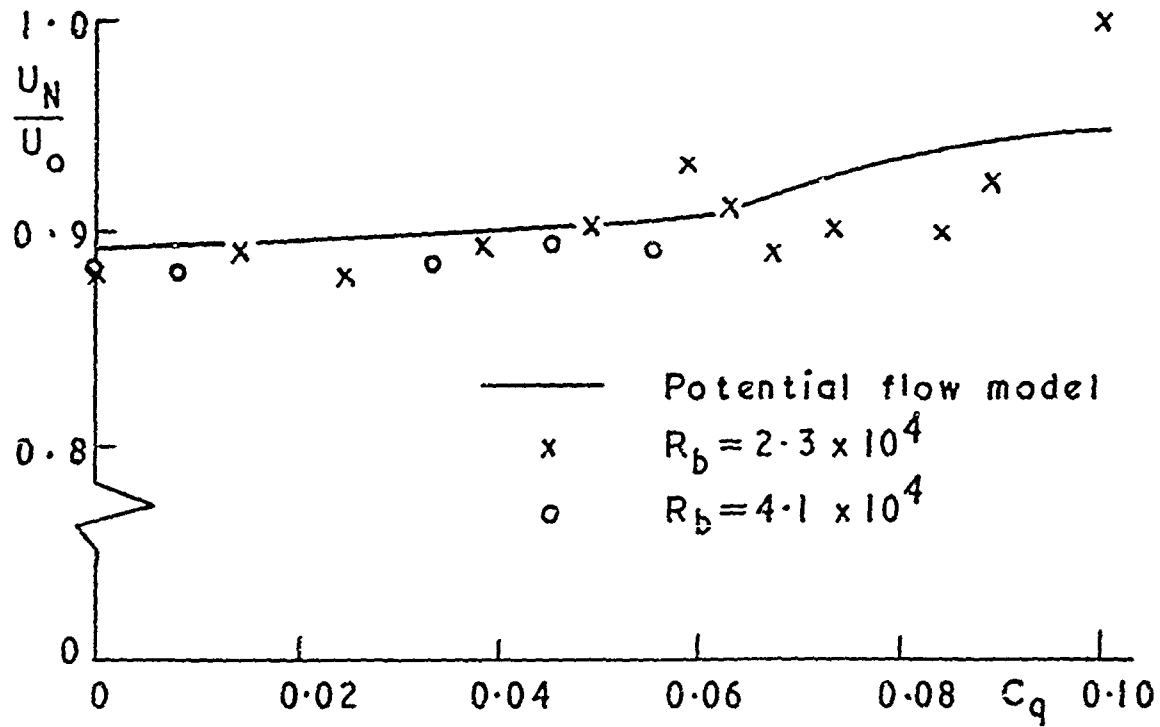
U_N / U_o versus bleed rate, $d/h = 0\cdot93$

FIG.8

$b/_a$ versus U_s/U_o for the condition C_{DS} is a minimum

FIG.9
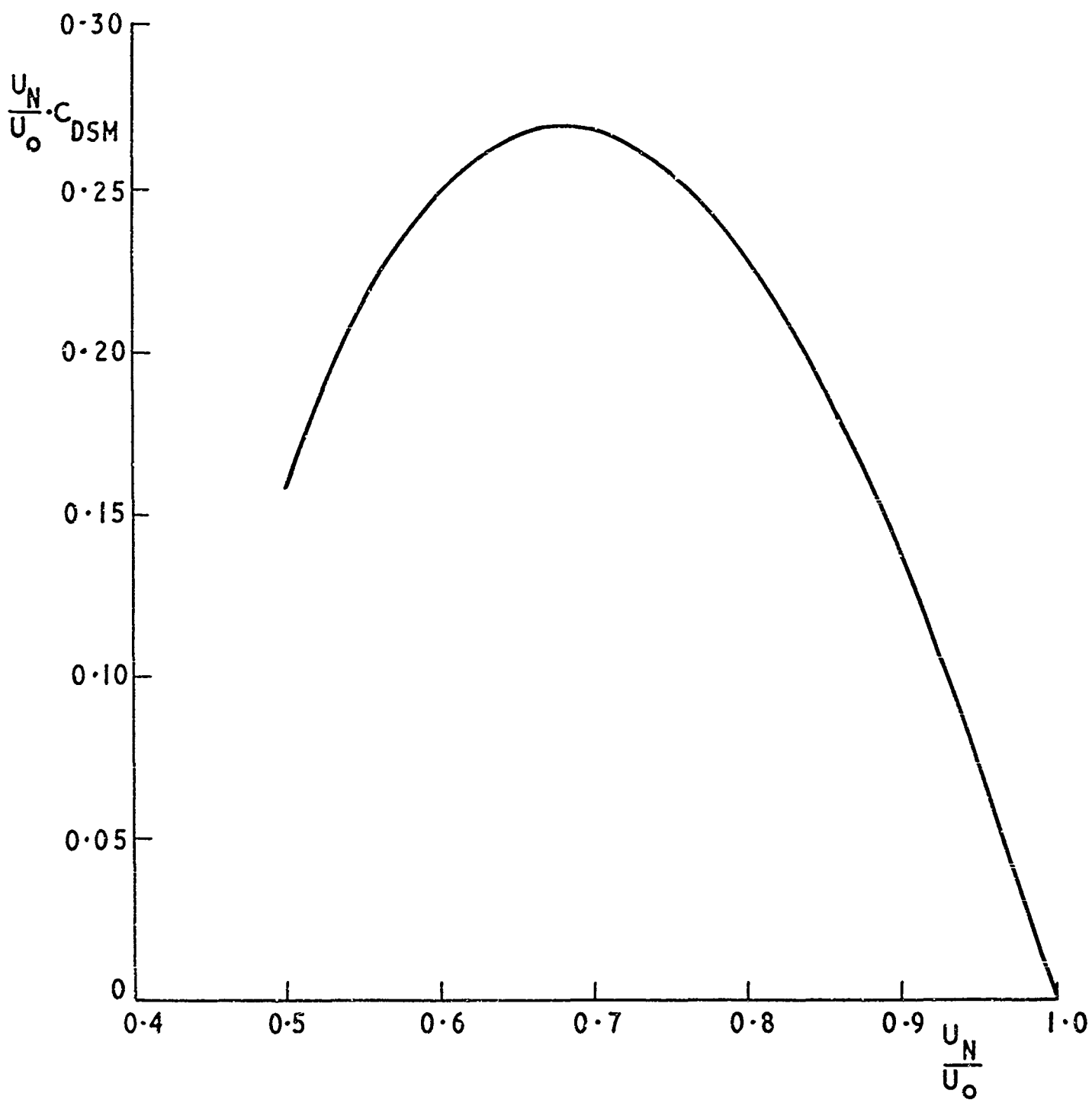
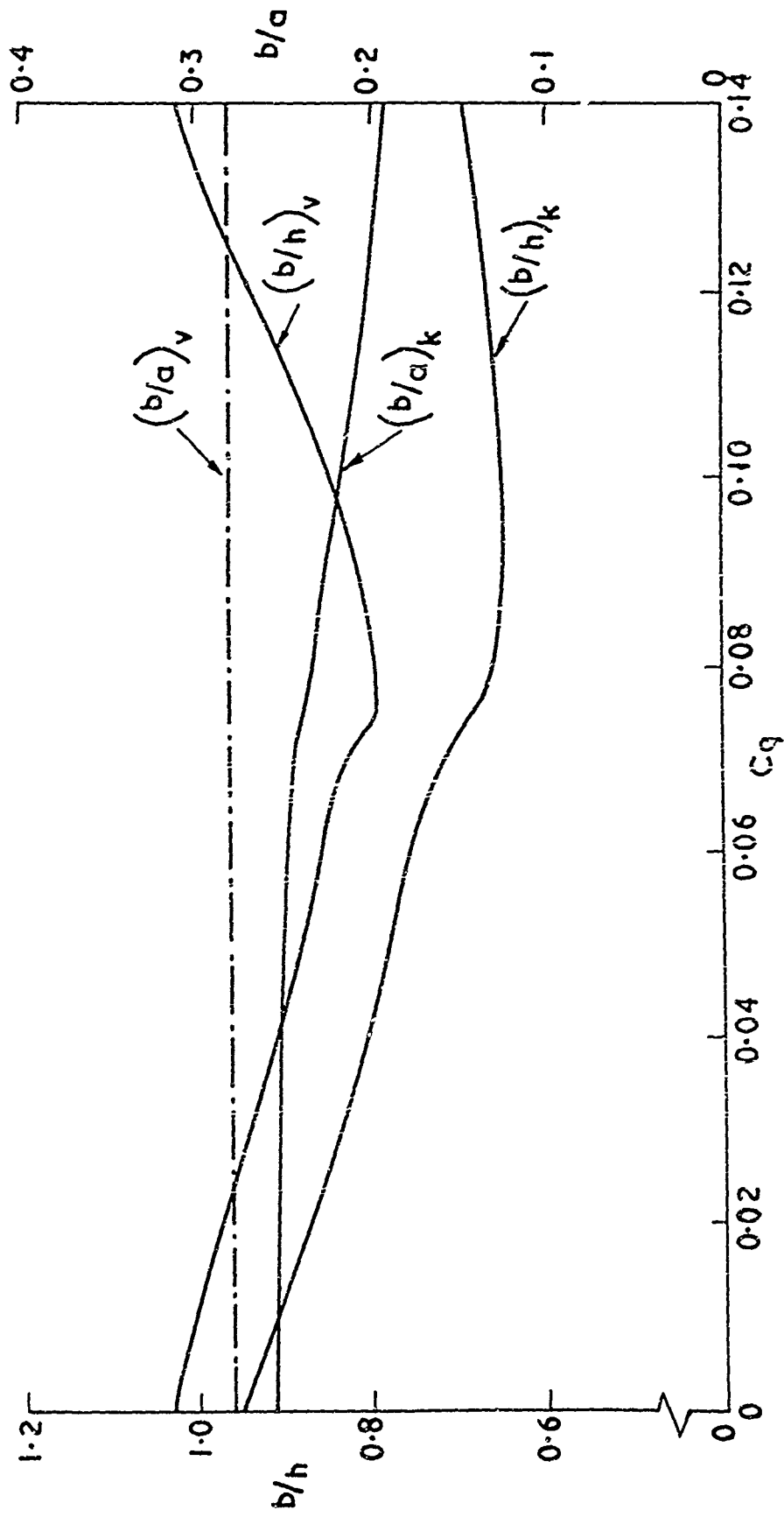$\dfrac{U_N}{U_o} \cdot C_{DSM}$ versus $\dfrac{U_N}{U_o}$

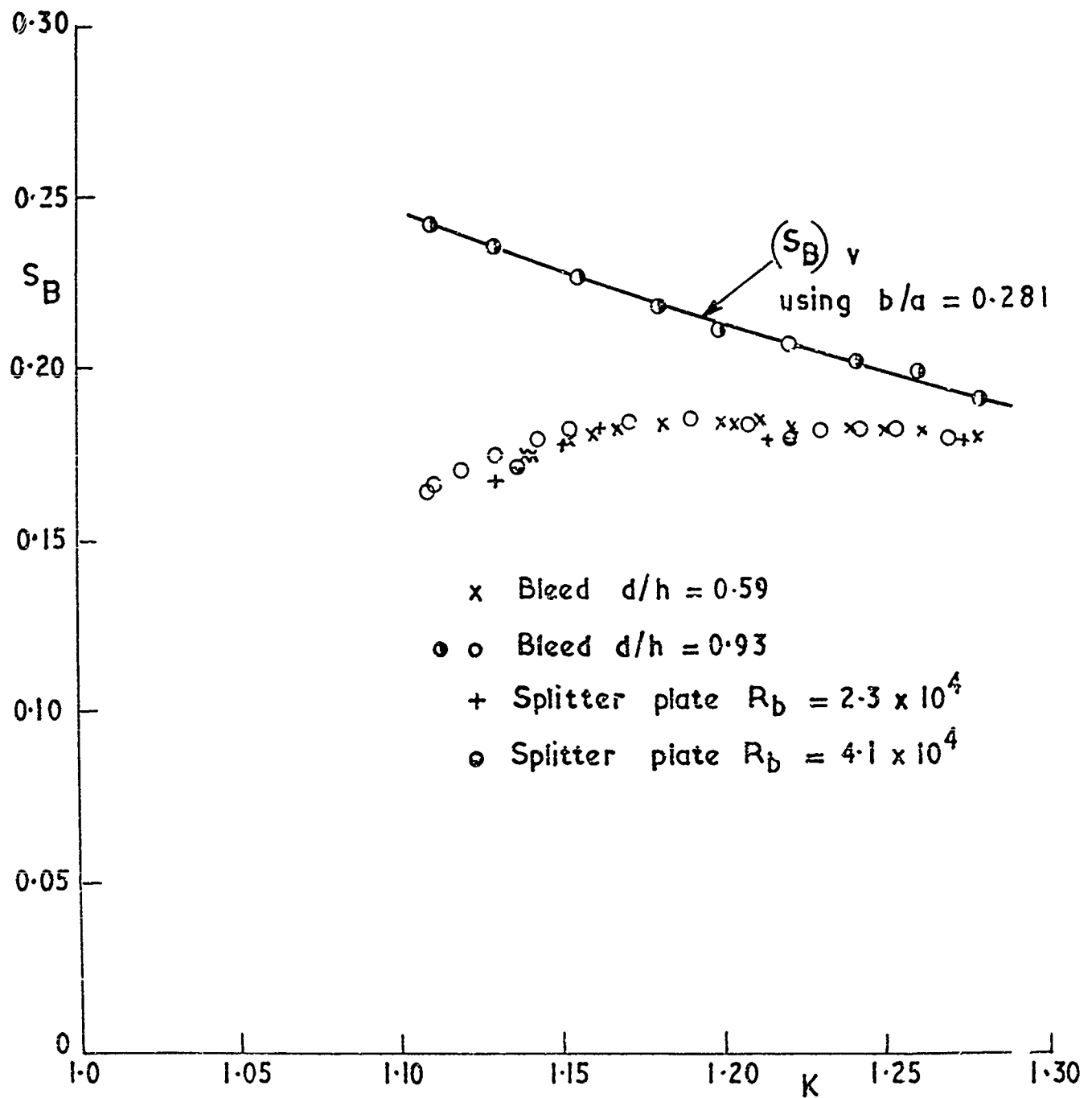# FIG. 10
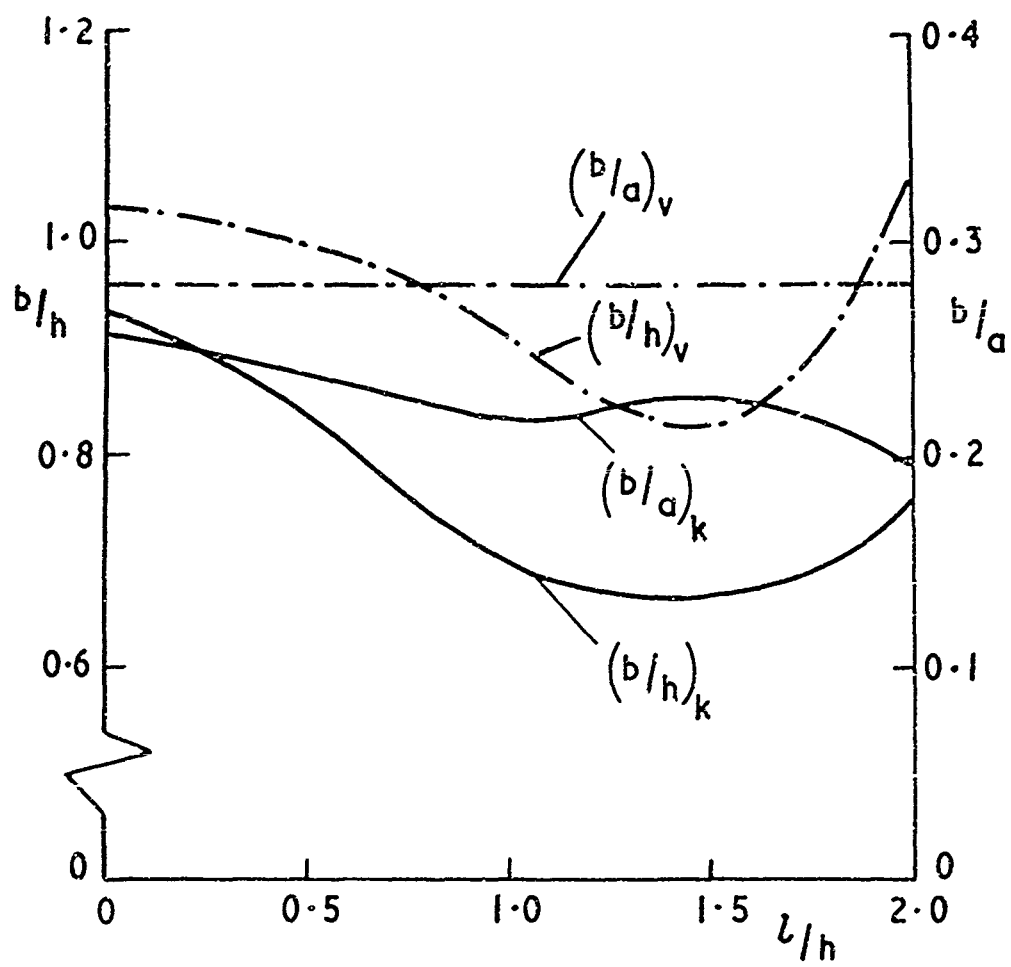
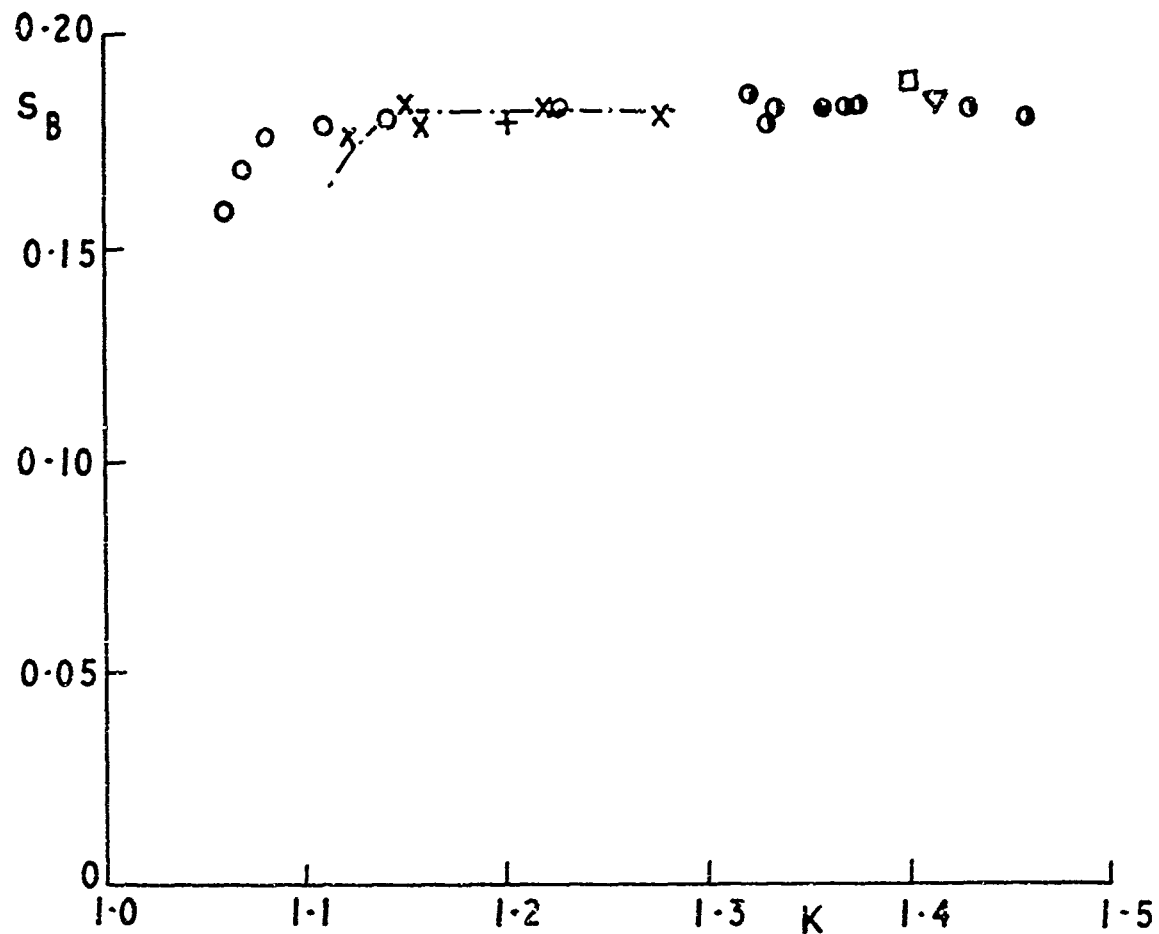Splitter plates—estimation of b/a and b/h at $R_b = 2 \cdot 3 \times 10^4$

FIG. 11

Base bleed — estimation of b/a and b/h, $d/h = 0.93$

FIG.12

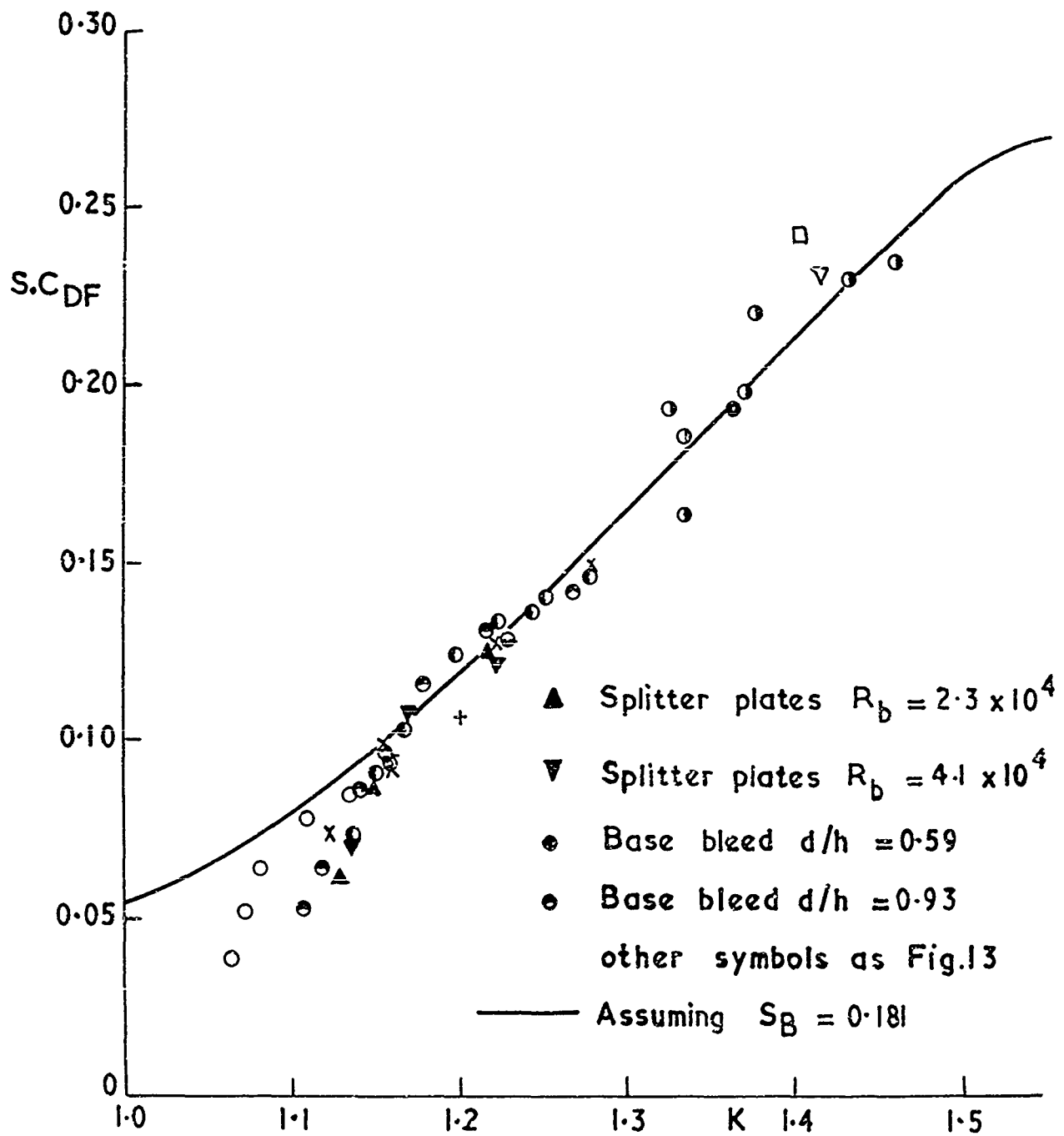S_B versus K for the base bleed and splitter plate results

x   Bleed   d/h = 0.59

o o Bleed   d/h = 0.93

+   Splitter   plate R_b = 2.3 x 10^4

o   Splitter   plate R_b = 4.1 x 10^4

$(S_B)_v$ using b/a = 0.281

FIG.13

S_B versus K for various bluff body shapes

x   splitter plates, Nash et al.(1963) Mach No. 0 4
o   base bleed, Wood (1964) and Bellhouse and Wood (1965)
●   ogival shape, Fage and Johansen (1927)
+   extended ogival shape, Fage and Johansen (1927)
∇   90° wedge, Roshko (1954(b))
□   flat plate, Roshko (1954(b))
o   circular cylinder, $R = 10^2$ to 10^5, Kronauer (1964)
●   circular cylinder, $R = 2 \times 10^6$ to 10^7, Roshko (1961)
—·—·   mean of results from Fig. 12

FIG.14

S.C$_{DF}$ versus K for various bluff body shapes